14th International Particle Accelerator Conference,Venice, Italy JACoW Publishing
ISBN: 978-3-95450-231-8 ISSN: 2673-5490 doi: 10.18429/JACoW-IPAC2023-THPM121

CONSTRUCTION OF AND EXPERIMENTS WITH A COMPACT PLASMA SOURCE

D. Chow*, N. Majernik†, P. Manwani‡, G. Andonian and J. Rosenzweig
University of California Los Angeles, Los Angeles, United States

Abstract

A versatile capillary discharge plasma source has been built and tested at UCLA for use in plasma wakefield experiments at the MITHRA and AWA facilities. This 8 cm long source can produce plasmas spanning multiple decades of density, enabling a range of experiments from the study of planetary plasmas to plasma wakefield accelerators (PWFA). The 3 mm aperture permits the propagation of high aspect ratio beams while the broad density tunability enables a detailed investigation into the transition between linear and nonlinear PWFA regimes. This paper will discuss the construction and testing of this capillary discharge plasma source and the use of an interferometric diagnostic system to measure plasma density.

INTRODUCTION

Versatile and compact plasma sources with precision density control have various applications such as plasma wakefield acceleration (PWFA) and simulating space radiation for instrumentation. In this paper, we describe the development of a capillary discharge plasma source, based on the design put forth in [1], that utilizes spontaneous breakdown of Argon gas to generate plasmas with on axis densities in the range of 10^{13}cm^{-2} to 10^{17}cm^{-2}. The capillary discharge system is designed and constructed with the initial intent of studying PWFA beam dynamics at the Argonne Wakefield Accelerator (AWA) at the Argonne National Laboratory, with special shaping of drive beam temporal and transverse distributions that allows for a wide range of beam-plasma experiments [2–4]. In this scheme, plasma is generated by injecting Argon gas into a ceramic (Macor) structure through two fill lines that feed into the main capillary initially at UHV levels. The gas then distributes along the capillary in an approximately bi-Gaussian pattern longitudinally (z-axis of the capillary). Plasma formation is motivated by the process of electrical breakdown which creates a msec-scale plasma channel from the injected Argon gas. This breakdown is characterized by Paschen's Law Eq. (1), which informs the voltage necessary for plasma production as a function of pressure (p), capillary length (d), secondary electron emission coefficient (γ_{se}), and two parameters A and B that must be experimentally determined for each system [5]. The behavior exhibited by Eq. (1) is plotted in Figure 1.

$$V_b = \frac{Bpd}{ln(Apd) - ln[ln(1 + \frac{1}{\gamma_{se}})]} \quad (1)$$

* drchow37@gmail.com
† nmajik@gmail.com
‡ pkmanwani@gmail.com

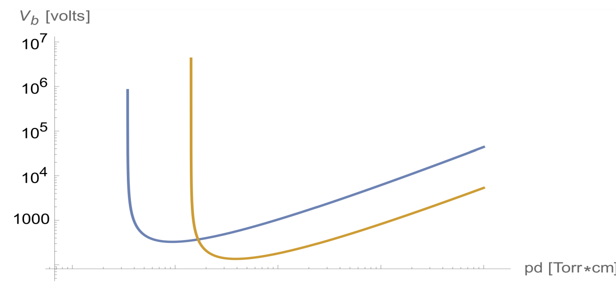

Figure 1: Example Paschen curves for Ne (blue) and He (orange).

In order to characterize the plasma source, we use a Michelson interferometer to measure on-axis plasma densities. The interferometer undegoes a phase shift from when the test arm is in vacuum to when the test arm includes propagation through the plasma. By measuring this phase shift directly, the plasma electron density, N_e, is calculated using

$$\int_{L_i}^{L_f} N_e \, dL = \frac{4\pi c^2 m_e \epsilon_0}{\lambda e^2} \Delta\phi \quad (2)$$

where λ is the laser wavelength, e is the electron charge, m_e is electron mass, and $L_f - L_i$ is the length of the capillary. This phase shift can also be interpreted as a change in the intensity of the interference pattern over a fixed area, which can be directly measured on an oscilloscope. For $N_e < 1 \times 10^{16}\text{cm}^{-2}$, Eq. (2) can be reduced to

$$\int_{L_i}^{L_f} N_e \, dL = 5.56 \times 10^{16} \frac{\Delta A}{A} \quad (3)$$

where ΔA is the amplitude of the interferometer signal when there is plasma in the test leg, and A is the amplitude of low frequency noise [6]. Most variation in the base interferometer signal comes from the physical vibration of optical elements due to external sources, such as the turbomolecular pumping system. However, the timescale of plasma formation and subsequent dissipation is much faster than physical vibration of the optical components, implying that ΔA and A should remain distinct for our experimental setup.

This paper will describe the physical setup of the capillary, interferometer and associated elements, and report on the initial results of the plasma characterization of the capillary discharge from benchtop measurments.

DESIGN

The fully assembled vacuum system along with the interferometer can be seen in Figure 2. The vacuum system consists of a main chamber with the ceramic structure inside,

ISBN: 978-3-95450-231-8 ISSN: 2673-5490 doi: 10.18429/JACoW-IPAC2023-THPM121

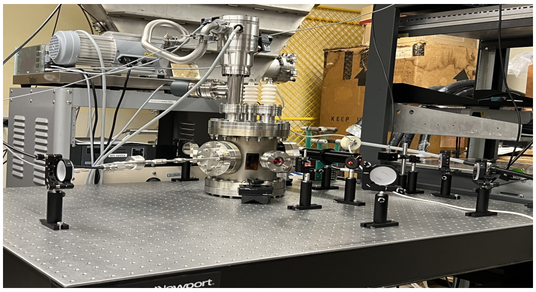

Figure 2: Vacuum chamber containing the plasma source along with an external interferometer for diagnosing plasma density.

and a gas intake that is regulated by a piezo-valve. The purpose of using a rapid valve is to decrease the gas load on the turbomolecular pumps, whilst maintaining UHV levels in the beamline. The rapid piezo-valve is connected to an electronic driver unit (EDU) that controls the rate of opening and closing of the valve, as well as the open and close duration times. The plasma chamber uses a turbomolecular pump that is backed by a diaphragm style roughing pump.The vacuum chamber is designed to accept two lamps for delivering high voltage pulses to the capillary. These lamps are connected to a 3 nF capacitor that discharges when the circuit is closed via a solid state switch. A system controller controls the discharge of argon into the Macor by triggering the EDU and the switch, which allows for precise selection of gas densities used for plasma formation.

The capillary is a cylinder of radius 0.15 cm bored out of the Macor that spans the length of the ceramic (8 cm). A picture of the Macor that houses the capillary is shown in Figure 3 alongside a CAD model that shows the main capillary channel and its fill lines. When under vacuum and with the piezovalve open, argon gas enters the capillary through these fill lines, dispersing along the length of the channel. Plasma formation is motivated by the sudden application of high voltage to the two ends of the capillary via electrodes connected to the lamps.

The Michelson interferometer is driven by a ThorLabs 633 nm, 5 mW, HeNe laser that comprises of two arms. The reference arm is always in atmosphere while the test arm passes through mediums of atmosphere, glass, vacuum, and plasma. The interference pattern is projected onto a photodiode connected to an osilloscope in order to measure the amplitude change in the interference pattern due the phase shifts incurred by plasma in the test arm.

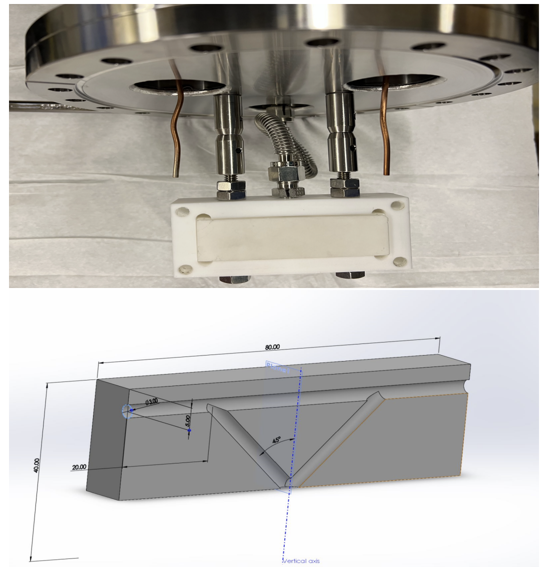

Figure 3: (Top) The mounting scheme of the Macor. Inside the chamber, wires are connected from the copper rods to the openings in the Macor. (Bottom) A CAD model of the interior of the Macor.

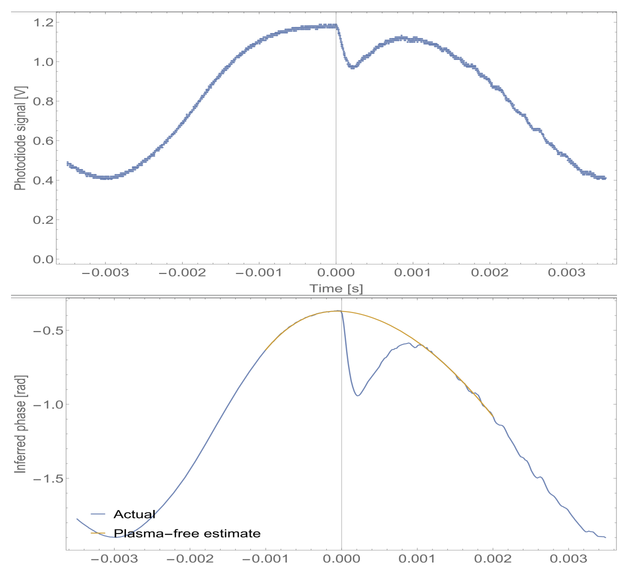

Figure 4: (Top) Signal from the photodiode vs time. A change in signal strength at t = 0 corresponds to a phase shift in the interferometer signal due to a changing path length in the test leg as a plasma forms. (Bottom) Conversion from amplitude to phase with a spline fit to the initial curve.

EXPERIMENTAL RESULTS

Testing of the plasma source has been in the context of determining functionality of the interferometer system. As such, we used arbitrary initial parameters for gas injection and breakdown. Measurements of plasma density have been performed on a single shot basis, where the piezo-valve is pulsed once per experiment and a single density profile measurement is taken in time. One such measurement can be seen in Figure 4, where the raw oscilloscope signal undergoes a noticeable shift during the formation of a plasma inside the capillary. To obtain on axis density vs time for this signal, we elected to convert the photodiode signal amplitude to signal phase and fit a spline to the plasmaless curve, which can also be seen in Figure 4. Applying Eq. (2) to each time step, we get Figure 5, which shows plasma den-

ISBN: 978-3-95450-231-8 ISSN: 2673-5490 doi: 10.18429/JACoW-IPAC2023-THPM121

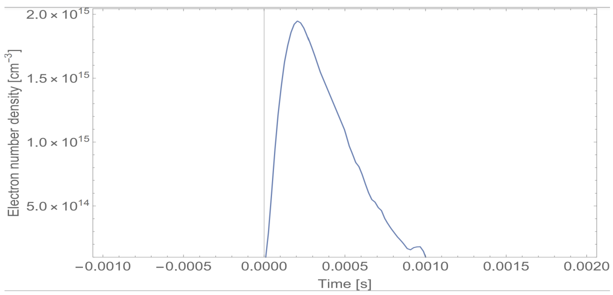

Figure 5: Plasma density vs time calculated using Eq. (3) using the data from Figure 4.

sity evolution in time and serves as a good baseline for what we expect future tests to look like.

CONCLUSION

We have presented a functioning compact plasma source that is capable of producing plasmas in a wide range of densities. An interferometer mounted outside the vacuum chamber housing the capillary allows for real time measurements of axial plasma density by analyzing the changing interference pattern over time. The preliminary results presented show proper function of the diagnostic system, and demonstrates its ability to measure the density of an arbitrary plasma. Development and testing of the capillary will continue before its eventual installation into the beamline at AWA.

REFERENCES

[1] S. Barber, "Plasma wakefield experiments in the quasi nonlinear regime," Jun. 2015. https://escholarship.org/uc/item/66k4r10w#main

[2] A. Fukasawa *et al.*, "Advanced Photoinjector Development at the UCLA SAMURAI Laboratory", in *Proc. IPAC'21*, Campinas, Brazil, May 2021, pp. 2728–2731. doi:10.18429/JACoW-IPAC2021-WEPAB056

[3] P. Manwani *et al.*, "Simulations for the Space Plasma Experiments at the SAMURAI Lab", in *Proc. NAPAC'22*, Albuquerque, New Mexico, USA, Aug. 2022, pp. 539–541. doi:10.18429/JACoW-NAPAC2022-TUPA87

[4] "Asymmetric Beam Driven Plasma Wakefields at the AWA", in *Proc. IPAC'21*, Campinas, Brazil, May 2021, pp. 1732–1735. doi:10.18429/JACoW-IPAC2021-TUPAB147

[5] M.A. Lieberman, A.J. Lichtenberg, "Direct Current (DC) Discharges", in *Principles of Plasma Discharges and Materials Processing*, John Wiley & Sons, Ltd, 2005, ch. 14, pp. 535–569. doi:10.1002/0471724254.ch14

[6] I. V. Lisitsyn, S. Kohno, T. Kawauchi, T. Sueda, S. K. S. Katsuki, and H. A. H. Akiyama, "Interferometer measurements in pulsed plasma experiments," *Japanese Journal of Applied Physics*, vol. 36, p. 6986, 1997. doi:10.1143/JJAP.36.6986